

Effect of complete oxidation on the vibrational properties of aluminum oxide thin films: An electron-energy-loss-spectroscopy study

P. J. Chen,* M. L. Colaianni, and J. T. Yates, Jr.

Surface Science Center, Department of Chemistry, University of Pittsburgh, Pittsburgh, Pennsylvania 15260

(Received 19 September 1989; revised manuscript received 2 January 1990)

The vibrational properties of ultrathin (8–15 Å) aluminum oxide films deposited on a Mo(110) substrate are studied with use of high-resolution electron-energy-loss spectroscopy (EELS) under specular-scattering conditions. It is found that remarkable intensity changes in the low-frequency (400-cm^{-1}) optical-phonon mode can be induced by varying the extent of oxidation in the thin film. Two types of characteristic phonon energy-loss spectra are obtained from EELS measurements, which correspond to Al-rich nonstoichiometric films and fully-oxidized aluminum oxide films, respectively. Conversion between the two types of oxide films can be achieved by chemical means. By means of combined EELS and Auger-electron-spectroscopy studies, spectroscopic criteria for complete oxidation are provided for the aluminum oxide thin films. Possible structure changes following the process of complete oxidation are discussed.

I. INTRODUCTION

The oxidation process on metal surfaces has traditionally been an active area of surface-spectroscopic investigation due to the importance of metal oxidation in metallurgy, catalysis, electrochemistry, and other technologies. In the case of an oxide thin film on a bulk metal, a "metal-rich" oxide is expected, or in other words, the oxide is produced in a metallic environment. For the spectroscopic investigation of oxidation, techniques such as Auger-electron spectroscopy (AES) and x-ray photoelectron spectroscopy (XPS) are often employed. In these investigations, the existence of a "metal background" sometimes interferes, making it very difficult to address such issues as completeness of oxidation, structural and chemical properties of the oxide film, etc.

It is therefore interesting to compare, for example, the vibrational properties of a pure oxide with that of an oxide in a metallic environment. Deposition of thin metal or metal oxide films on a carefully chosen substrate may provide an alternate method in which the overlayer-metal-oxide properties can be separated from that of the substrate under favorable conditions. In the past, high-resolution electron-energy-loss spectroscopy (EELS) has been successfully used to study the oxidation of metals and the vibrational spectrum of metal oxides.^{1–7} Recently, EELS has also been used to study the vibrational properties of ultrathin metal films, such as the ordered Ni film deposited on a Cu(100) substrate.⁸

High area aluminum oxide has been used traditionally as a supporting material in catalytic chemistry.⁹ Aluminum oxide thin films, either grown on Al metal or vapor deposited on a substrate, have been used recently in the study and modeling of supported metal catalysts where the metal is deposited by evaporation in ultrahigh vacuum on the oxide film.^{10–12} A fundamental understanding of the properties of the oxide film, especially the vibrational properties, is of considerable importance to the research of this type.

The oxidation of aluminum has been extensively studied in the past.¹³ An appreciable amount of experimental work has been carried out on oxidized aluminum single crystals using AES,¹⁴ surface extended x-ray absorption fine structure SEXAFS,^{15,16} photoemission,^{17–21} ion scattering,²² inelastic electron tunneling,²³ infrared spectroscopy^{24,25} and EELS.^{5–7,26–30} Experimental investigations of the vibrational properties of aluminum oxide films supported on different substrate materials, such as Si and Au, have also been reported previously, using the reflection ir absorption method.³¹ However, most of these vibrational investigations were performed with rather degraded resolution—possibly due to the inhomogeneity associated with the rather thick Al_2O_3 films used. Also, due to the limited spectral range in ir measurements, the observation of low-frequency ($\sim 600\text{ cm}^{-1}$ or lower) vibrational modes in oxide thin films is severely hindered. On the other hand, little work of the type reported here has been due to exploit the sensitivity and spectral range of EELS to characterize the vibrational properties of deposited aluminum oxide thin films on inert substrate materials.

In this paper we present an Auger-electron-spectroscopy and high-resolution electron-energy-loss-spectroscopy study of the vibrational properties of ultrathin (a few monolayers) aluminum oxide films deposited on a Mo(110) single crystal surface. We show that remarkable changes in the optical-phonon mode spectrum in the thin film can be induced by varying the extent of oxidation in the oxide.

II. EXPERIMENT

Experiments were carried out in a stainless-steel UHV chamber described previously.⁶ The typical base pressure of the UHV system was lower than 1×10^{-10} mbar. The apparatus is equipped with a single-pass cylindrical-mirror-analyzer (CMA) Auger optics and a Leybold-Heraeus ELS-22 spectrometer for high-resolution

electron-energy-loss-spectroscopy studies. EEL spectra were recorded in the specular direction at an incident electron beam energy of 3.8 eV. The typical resolution [full width at half maximum (FWHM)] for the $\text{Al}_2\text{O}_3/\text{Mo}(110)$ system was $80\text{--}100\text{ cm}^{-1}$ at an elastic beam counting rate of 1×10^5 cps. Auger measurements were recorded in the $dN(E)/dE$ mode at a primary beam energy of 3 keV, a modulation voltage of 3.0 V_{p.p.}, and a total electron current of $3\ \mu\text{A}$ at the crystal. Both EEL and Auger measurements were performed with the substrate below 150 K. The digitally recorded EEL spectra in this work were processed by a Fourier filtering method³² to improve the signal-to-noise ratio.

The Mo(110) single crystal was oriented, polished, and mounted with standard procedures³³ for cooling to 90 K and heating to 1400 K by passing current through 0.25-mm-diam W support wires. The cleanness of the Mo(110) surface is assured by Auger electron spectroscopy. The aluminum evaporation source was built by winding Al wire (Goodfellow Advanced Materials, 99.99+%) on tungsten filaments which could be resistively heated. Aluminum oxide deposition was achieved by evaporating Al in the presence of O_2 gas (Linde, 99.999+%) with the Mo(110) substrate at $\sim 90\text{ K}$ for all depositions. The oxide film was generally annealed at 1200 K in vacuum for typical times of 30 min to 1 h to order and stabilize the structure before EEL and Auger spectra were taken. By controlling the O_2 pressure during deposition, films with different degrees of oxidation were obtained. The typical rate of oxide deposition was $2\text{--}3\ \text{\AA}/\text{min}$. The formation of the aluminum oxide was monitored by AES, and the thickness of the oxide layer determined by measuring the attenuation of the Mo(MNN) Auger transition signal at 186 eV. The oxide thin film can be made with very good reproducibility at a typical thickness of $8\text{--}15\ \text{\AA}$. This thickness is ideal for EELS measurements since a thicker layer would undergo charging resulting in a decrease of EEL spectral resolution. With the detection limit of EELS (better than 1% for CO), no CO adsorption on the oxide film was detected at 90 K following a 7.5 L CO exposure ($1\ \text{L} = 1\ \text{langmuir} = 1 \times 10^{-6}\ \text{torr sec} = 3.8 \times 10^{14}\ \text{CO}/\text{cm}^2$), which indicates that aluminum oxide, in the thickness range mentioned above, covers the Mo(110) completely.

It has been shown through photoemission,^{17,21} x-ray diffraction,³¹ SEXAFS,¹⁵ and slow positron³⁴ studies that amorphous aluminum oxide experiences a phase transition from an amorphous to a crystalline ($\gamma\text{-Al}_2\text{O}_3$ -like) phase over a rather wide temperature range from 650 to 1300 K. Our EELS studies also indicate that a major structural change occurs upon heating the oxide layer (Fig. 1). Codeposition of aluminum and oxygen at 110 K resulted in amorphous or poorly ordered aluminum oxide as the EEL spectrum [Fig. 1(a)] shows only a broad pair of loss feature at around 790 cm^{-1} and 1445 cm^{-1} , although AES clearly showed that oxidation of Al^0 had occurred. Upon heating the codeposited oxide layer to 700 K or above, the amorphous-to-crystalline transition occurs as indicated by the marked change in the EEL spectra [Figs. 1(b) and 1(c)], resulting in distinct energy-loss features. It is probably not necessary for a long-

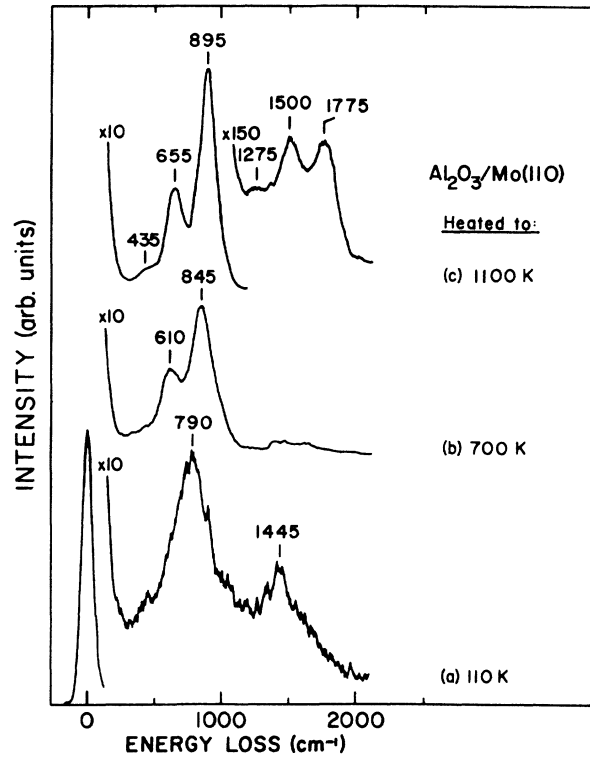


FIG. 1. Al_2O_3 formation on Mo(110) as a function of substrate temperature; EEL spectra showing the development of energy-loss features upon heating: (a) after codeposition of aluminum and oxygen on Mo(110) at 110 K; (b) after heating to 700 K; (c) after heating to 1100 K.

range ordering in the crystal structure to be present in order to produce the distinct energy-loss spectrum. Therefore the term "crystalline" oxide may not involve very long-range ordering, although definite information about the range of order is not available. The extended temperature range available for heating the oxide film on the Mo substrate, which is unattainable on Al single crystals due to the low melting point of Al, facilitates the structural development of the aluminum oxide. Direct x-ray diffraction measurement has been carried out by Brüesch *et al.*³¹ in their study of a sputter-deposited aluminum oxide thin film on Si(111) wafers, where the $\gamma\text{-Al}_2\text{O}_3$ structure was confirmed after heating to 1300 K. Also, it is observed that diffusion between substrate Mo and the thin film of aluminum oxide did not pose a problem in our temperature range as judged from the Auger spectra taken before and after annealing. There was no clear EELS evidence for molybdenum oxide formation in the same temperature range, nor for Mo migration into the Al_2O_3 film.

III. RESULTS AND DISCUSSION

A. Brief summary of previous results

Before proceeding with the experimental observations, it is useful to briefly summarize the results of previous

EELS studies of the vibrational properties of aluminum oxide thin films formed on aluminum single crystal surfaces. It should be kept in mind that all the EELS results referred to here are recorded under specular-scattering conditions which reflect only the dipole active optical-phonon modes at the center of surface Brillouin zone (SBZ), $\bar{\Gamma}$.

EELS studies of the vibrational properties of aluminum oxide have been carried out on single crystal aluminum surfaces oriented in $\langle 111 \rangle$ and $\langle 100 \rangle$ crystallographic directions.^{5-7,26-30} For oxide layers of 5–10 Å thickness, the results from EELS experiments on both surfaces were very similar, namely, there are three distinct energy-loss features located at ν_1 , 325–430 cm^{-1} ; ν_2 , 625–650 cm^{-1} ; and ν_3 , 820–880 cm^{-1} . Figure 2 shows the EEL spectrum of the oxide film on an Al(111) surface recorded in our earlier work under specular-scattering conditions.⁷ The assignment and interpretation of these loss features was primarily based on the lattice dynamical model calculation of Erskine, Strong, and co-workers.⁵ Their calculation employed a slab model of Al and O with parametrized force constants. Dipole active optical-phonon frequencies at the center of the surface Brillouin zone, $\bar{\Gamma}$, were calculated with the set of force constants best fitted to the observed vibrational frequencies. According to the results of the calculation (see inset, Fig. 2), the high-frequency loss mode ν_3 was attributed to a vertical vibrational motion in which the displace-

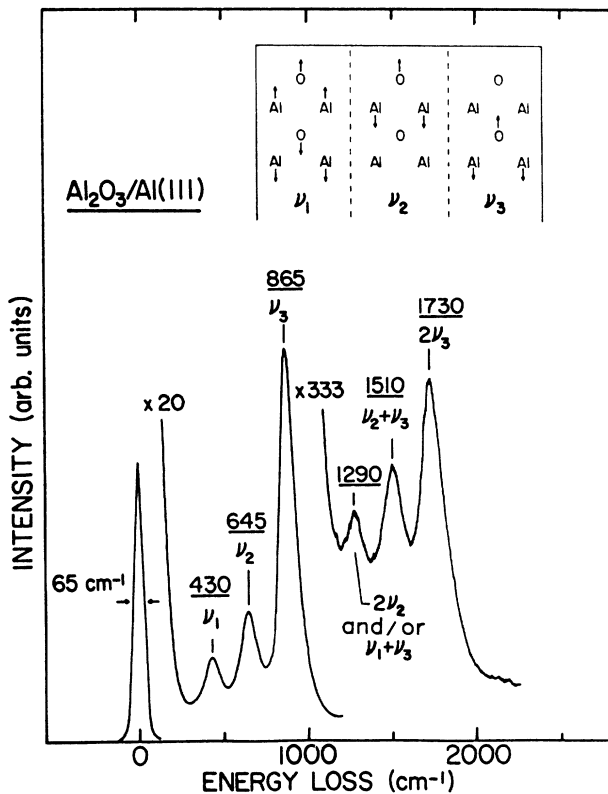


FIG. 2. EEL spectrum of an oxidized Al(111) surface (Ref. 7) and the schematic diagram indicating the mode assignments by Erskine and Strong (Ref. 5). Oxide thickness $d = 5$ Å.

ment of the oxygen underlayer and the subsurface Al plane are 180° out of phase. The mode ν_2 at 645 cm^{-1} was attributed to a similar motion involving the oxygen overlayer and the surface Al plane. Finally, the low-frequency feature ν_1 at 430 cm^{-1} was considered to involve the oxygen overlayer and surface Al plane as a slab moving together, 180° out of phase against the slab composed of the oxygen underlayer and subsurface Al plane. It is this last mode, ν_1 , that is of particular importance to our current experimental studies. In addition to the fundamental vibrational modes discussed, double loss modes are clearly observed at higher energies as seen in Fig. 2.⁷ It should be noted that although the Erskine-Strong work was modeled for an oxidized Al(111) surface, the EELS experimental results on an oxidized Al(100) surface²⁹ yielded essentially the same loss frequencies and intensity pattern, which is an indication of similar oxide formation on both surfaces. It is likely that once the oxide phase forms through the penetration of O atoms into the crystal lattice, there is little difference in the nature of the bulk oxide film formed on different Al crystal planes.

B. EELS studies on Al_2O_3 films on Mo(110)

1. Optical-phonon modes observed in EELS

Figure 3(a) shows the EEL spectrum of the phonon modes in an aluminum oxide thin film made under the deposition condition of 5×10^{-8} mbar O_2 . The low-frequency phonon mode at ~ 400 cm^{-1} , normally seen on oxidized aluminum single crystal surfaces, is almost completely absent. The double loss region (1000–2000 cm^{-1}) also exhibits a distinctive combination arising from ν_2 and ν_3 , the two primary loss modes: $2\nu_2$, $\nu_2 + \nu_3$, and $2\nu_3$. AES measurements indicate complete oxidation of Al as signified by the presence of the 54-eV $\text{Al}^{3+}(L_{2,3}VV)$ transition and the absence of the 68-eV $\text{Al}^0(L_{2,3}VV)$ transition. We believe the two-phonon-mode film represents a limiting condition most likely corresponding to Al_2O_3 , beyond which further oxidation treatment does not bring any changes to the oxide. Therefore it is referred to as “stoichiometric Al_2O_3 .”

Figure 3(b) shows the EEL spectrum of the phonon modes of an aluminum oxide thin film deposited under reduced O_2 pressure (1×10^{-8} mbar or less). The spectrum resembles that of oxidized Al single crystal surfaces as may be seen by comparison with Fig. 2; i.e., three phonon modes are present with their frequencies at 400, 620, and 850 cm^{-1} . This similarity is further confirmed by the very similar double loss spectra in Figs. 2 and 3. AES measurements indicate the presence of elemental Al^0 in the film as signified by the simultaneous presence of the 68-eV Al^0 and 54-eV $\text{Al}^{3+}(L_{2,3}VV)$ Auger transitions [as will be shown in Fig. 5(a)]. We will refer to such an aluminum oxide film exhibiting a three-phonon loss feature as “nonstoichiometric” or Al-rich aluminum oxide.

2. Conversion between the two types of thin films

Since there is only one oxidation state of aluminum as shown by photoemission studies,^{18,20} the above results

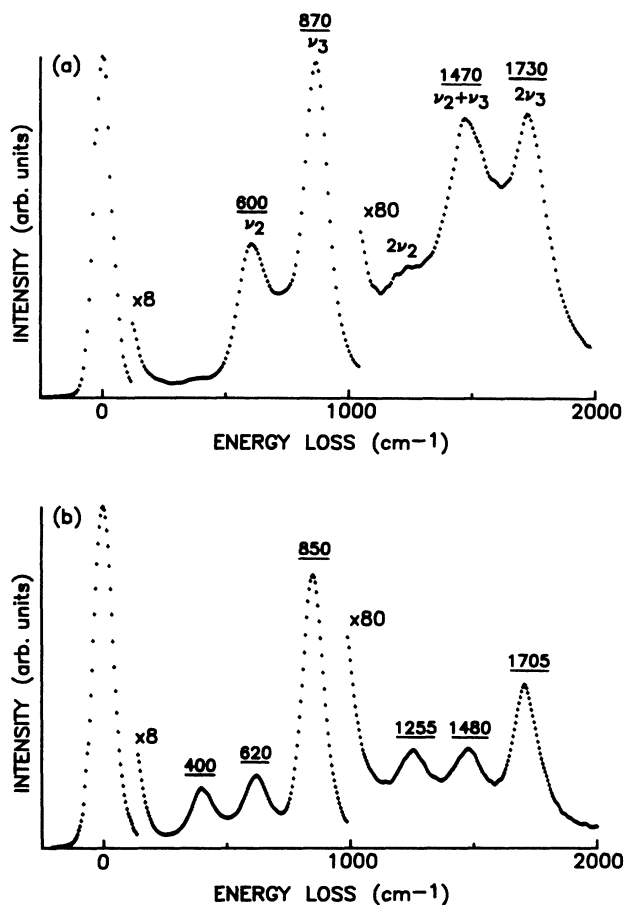


FIG. 3. EEL spectra of (a) fully oxidized Al₂O₃ (heavy oxidation) and (b) Al-rich Al₂O₃ thin films on the Mo(110) substrate (light oxidation).

strongly suggest that the presence of elemental Al⁰ in the aluminum oxide thin film is responsible for the phonon mode at 400 cm⁻¹. To prove this point, experimental attempts were made to further oxidize the Al-rich oxide film of Fig. 3(b) and, therefore, to achieve conversion between these two types of oxide films. Figure 4 shows the EELS result after exposing the nonstoichiometric Al₂O₃ layer to a total oxygen fluence of 1 × 10¹⁶ molecules/cm² at 1200 K through a calibrated microcapillary array molecular beam doser.³⁵ It is clearly evident that the 400-cm⁻¹ mode was completely removed in producing the more heavily oxidized film. A significant increase in the ν₂ relative intensity (~600 cm⁻¹) accompanied by a small shift toward lower frequency was also found, which may indicate a structural rearrangement in the oxide thin film.

Finally, as shown in Fig. 4(c), on this fully oxidized Al₂O₃ film, additional deposition at 90 K of Al metal of about 3 Å thickness, followed by annealing at 1200 K, resulted in the regeneration of the ν₁ mode (~400 cm⁻¹). Auger measurement indicated the presence of elemental Al⁰ in the oxide film after annealing. It is clear that a small amount of Al metal has become incorporated into the oxide lattice, most probably through diffusion during

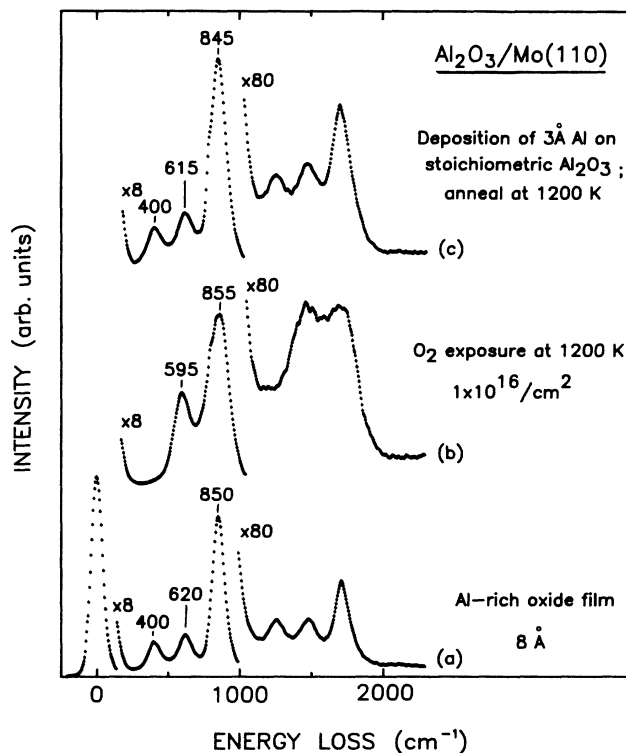


FIG. 4. EEL spectra showing the conversion between the three- and two-phonon-mode oxide thin films: (a) Al-rich aluminum oxide thin film of 8 Å thickness; (b) after 1 × 10¹⁶/cm² O₂ exposure at 1200 K; (c) after 3-Å metallic aluminum deposition on top of a stoichiometric Al₂O₃ film at 90 K and 5 min annealing at 1200 K.

annealing at elevated temperature, since at 1200 K the Al overlayer would be expected to simply evaporate in vacuum. The excessive metallic aluminum in the oxide film resulted in changes in its vibrational spectrum. Thus the aluminum oxide film can be controlled between the two conditions either through addition of Al or through heavy oxidation.

To better follow the conversion from the Al-rich nonstoichiometric aluminum oxide to stoichiometric Al₂O₃, Auger measurements were also made along with EELS. Figure 5(a) shows an Auger spectrum of an Al-rich Al₂O₃ thin film exhibiting both Al(L_{2,3} VV) transitions at 68 eV (elemental Al⁰) and 54 eV (Al³⁺). Reactive sputter-implantation of O₂⁺ on the Al-rich thin film was attempted in order to achieve, by another route, the complete oxidation of the residual Al⁰ incorporated in the oxide lattice. This was proven more efficient in carrying out complete oxidation than the O₂ molecular beam method just mentioned, especially for thick oxide films. O₂⁺ ions of 1 keV were produced from a commercial sputter gun and used to carry out reactive sputtering with the Al-rich oxide thin film on the Mo substrate at 90 K. The effect of further oxidation of the Al-rich thin film was monitored by AES [Figs. 5(b)–5(g)]. The gradual removal of metallic Al in the thin film as a result of O₂⁺ implantation was observed at various levels of reactive O₂⁺ sputtering.

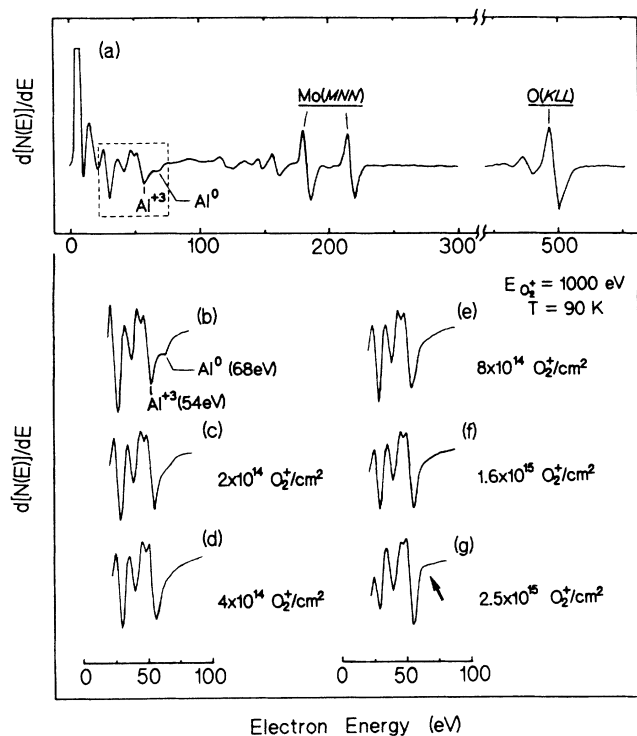


FIG. 5. Auger electron spectra of $\text{Al}_2\text{O}_3/\text{Mo}(110)$ showing the removal of residual metallic Al^0 (68 eV) by reactive O_2^+ sputtering: (a) Al-rich aluminum oxide thin film of 8-Å thickness; (b) same as (a), expanded region of 0–100 eV; (c) after $2 \times 10^{14} \text{ O}_2^+/\text{cm}^2$; (d) after $4 \times 10^{14} \text{ O}_2^+/\text{cm}^2$; (e) after $8 \times 10^{14} \text{ O}_2^+/\text{cm}^2$; (f) after $1.6 \times 10^{15} \text{ O}_2^+/\text{cm}^2$; (g) after $2.5 \times 10^{15} \text{ O}_2^+/\text{cm}^2$.

The gradual disappearance of the 68-eV $\text{Al}^0(L_{2,3}VV)$ Auger transition and the change in line shape in the 54–68 eV region clearly indicates the progressive oxidation of the residual elemental Al. In their AES studies of aluminum oxide thin films deposited on a W substrate, Madden and Goodman¹⁰ have also concluded that exposure to O_2 at elevated temperatures is necessary for complete oxidation of Al thin films on a W substrate. Our Auger spectrum of fully oxidized Al_2O_3 agrees very well with the spectrum of Madden and Goodman.¹⁰ However, in a similar AES and work function study of aluminum oxide films on a glass substrate, conducted earlier by Benndorf, Seidel, and Thieme,³⁶ there were signs of considerable residual metallic aluminum present in their oxidized films according to AES.

EELS measurements were also made at different levels of reactive O_2^+ sputtering (Fig. 6). The O_2^+ sputtered oxide film was annealed at 1200 K briefly prior to each EELS scan to reorder the surface. The EEL spectra show the gradual removal of the 400-cm^{-1} mode as oxidation is carried out. The following experimental observation is of considerable importance: the occurrence of a clear break on the high-energy side of the Al^{3+} 54-eV Auger peak [see arrow, Fig. 5(g)] is always accompanied by the presence of the characteristic two-phonon-mode EEL spectrum. We believe these two spectroscopic cri-

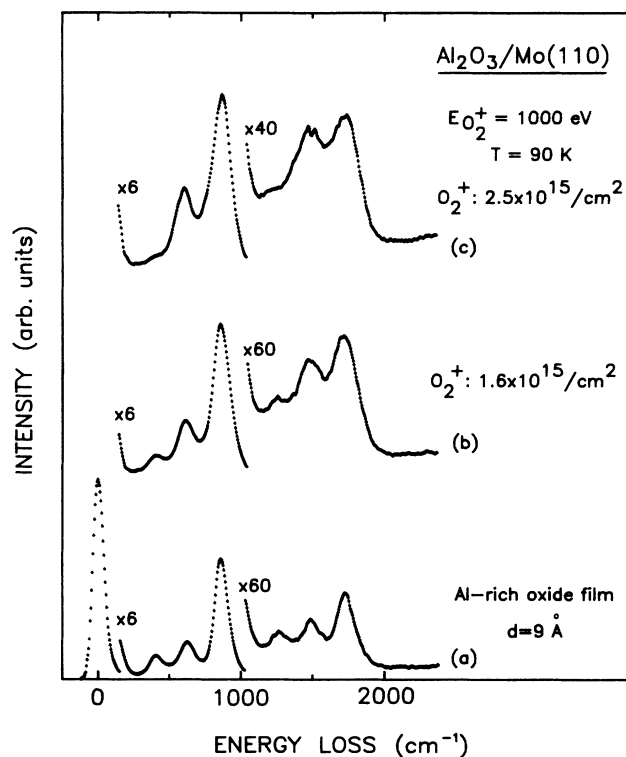


FIG. 6. The effect of reactive O_2^+ sputtering on the EEL spectrum of the aluminum oxide: (a) Al-rich aluminum oxide film of 9 Å thickness; (b) after $1.6 \times 10^{15} \text{ O}_2^+/\text{cm}^2$ sputtering and annealing at 1200 K for 5 min; (c) after $2.5 \times 10^{15} \text{ O}_2^+/\text{cm}^2$ sputtering and annealing at 1200 K for 5 min.

teria involving AES and EELS are an indicator of complete oxidation and should be considered as the definition of stoichiometric Al_2O_3 mentioned previously. It is clear that relatively minor differences in the Auger line shape near 60 eV are accompanied by rather strong differences in the EEL spectrum, suggesting that EELS is a more sensitive indicator of complete oxidation of Al to produce Al_2O_3 . These EELS and AES measurements provide convincing evidence about the origin and controlling factors responsible for the 400-cm^{-1} mode on the non-stoichiometric aluminum oxide thin film.³⁷

The effect of physical sputtering on the Al-rich oxide layer is shown in Fig. 7. These experiments were performed in order to exclude the possibility that *preferential sputtering* is responsible for the effects shown in Figs. 5 and 6. Controlled Ar^+ ion sputtering on the Al-rich oxide film resulted in partial removal of the oxide layer as would be expected. No signs of significant preferential sputtering were found as judged by AES. EELS studies on the Ar^+ -sputtered oxide film after annealing showed virtually no change in the characteristic three-phonon-mode spectrum down to the monolayer level despite the disorder-reorder caused by the Ar^+ sputtering-annealing cycles. This observation suggests that metallic Al^0 is uniformly distributed through the Al-rich aluminum oxide film.

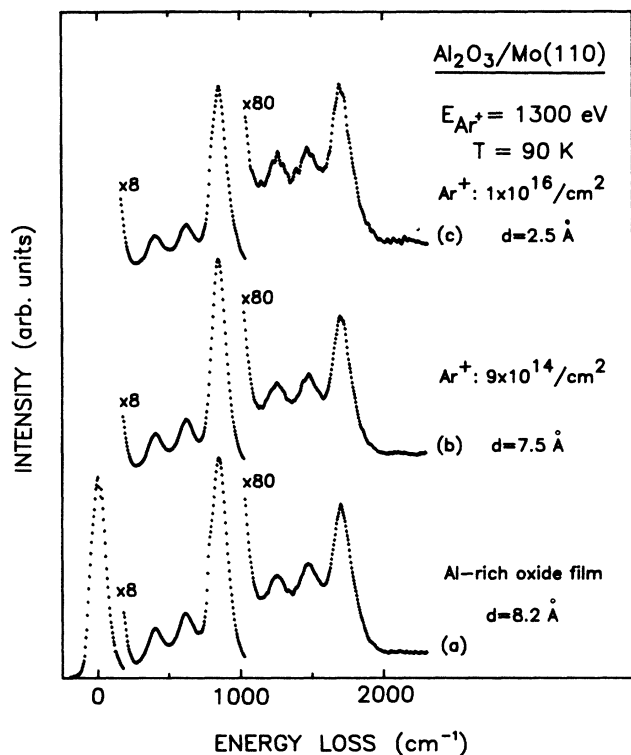


FIG. 7. The effect of Ar^+ sputtering on the EEL spectrum of the Al-rich aluminum oxide thin film: (a) initial oxide film of 8.2 Å thickness; (b) after $9 \times 10^{14}/\text{cm}^2$ Ar^+ sputtering and annealing at 1200 K for 5 min. Oxide thickness = 7.5 Å; (c) after $1 \times 10^{16}/\text{cm}^2$ Ar^+ sputtering and annealing at 1200 K for 5 min. Oxide thickness = 2.5 Å.

C. Possible origin of the 400-cm^{-1} phonon mode in Al-rich aluminum oxide

The basis for a comparison between the oxide formed on (1) single crystal aluminum surfaces and (2) the oxide formed from a thin film of Al, rests primarily on the fact that the oxide layer, upon annealing, undergoes an amorphous-to-crystalline transition, which, to first order, is independent of the details of the structure of the Al at the interface. According to the low-energy electron diffraction (LEED) study of Jackson and Hooker,³⁸ deposition of aluminum on Mo(110) results in epitaxially grown Al(111) films. We have deposited aluminum films on Mo(110) with subsequent mild oxidation. The resulting phonon spectra from EELS are virtually identical for Al-rich aluminum oxide thin films made by methods (1) or (2) above. Venus, Hensley, and Kesmodel observed a very similar phonon spectrum on oxidized polycrystalline Al foil.¹² Also, on oxidized Al(111) and Al(100) surfaces, very similar phonon spectra were recorded in EELS studies.^{5-7,29-30} Therefore, for an Al-rich oxide film, there is no evidence, as judged by EELS, of any differences in the vibrational spectrum of the films produced by different film preparation procedures or by choice of different substrates. This makes the comparison between Al single crystal work^{5-7,26-30} and the current work appropriate and meaningful. A basic finding from our work^{6,7} and

from the literature^{5,12,26-30} is that upon oxidizing aluminum single crystals under UHV conditions, one never obtains in EELS the two-phonon-mode spectrum characteristic of stoichiometric Al_2O_3 . The influence of excessive metallic aluminum prevails in these oxide films irrespective of the substrate crystal face involved.

There is little doubt about the origin of the 400-cm^{-1} mode in the Al-rich aluminum oxide film from our experimental findings. It is due to an Al^0 impurity in the Al_2O_3 film. The Erskine and Strong model for the 400-cm^{-1} mode attributes it to the vibration of a surface slab of Al^{3+} and O^{2-} ions, and this model was proposed on the basis of an ordered structure producing a (1×1) LEED pattern.

There is experimental evidence indicating that the species associated with the 400-cm^{-1} mode are not localized in the topmost atomic layer.^{28,30} For example, unlike the 625-cm^{-1} mode, the 400-cm^{-1} mode is not preferentially affected by monolayer adsorption²⁸ or by metal overlayer deposition.³⁰ In addition, the 400-cm^{-1} frequency is substantially higher than the maximum phonon frequency for clean aluminum or molybdenum surfaces; therefore the possibility of a resonant substrate phonon mode can be ruled out.³⁹

From a structural point of view, the requirement of stoichiometry and its consequences on crystal structure have to be properly considered here. In the situation of complete oxidation, stoichiometry requires certain structural changes or rearrangements. It is quite likely that the Erskine-Strong model is valid only for Al-rich nonstoichiometric oxide where the O^{2-} anions can arrange themselves in the high-symmetry (tetrahedral) interstitial vacancies of the fcc aluminum metal lattice according to the model⁵ and some supporting experimental evidence.^{15,16} This interstitial filling model provides the characteristic three-phonon-mode spectrum according to lattice dynamic calculations. In contrast to this, upon complete oxidation and annealing, the stoichiometric oxide exhibits structure of a different type, namely, $\gamma\text{-Al}_2\text{O}_3$, as suggested by many previous experimental findings.^{15-17,21,31} This can presumably produce the characteristic two-phonon-mode vibrational spectrum. In a $\gamma\text{-Al}_2\text{O}_3$ structure the O^{2-} cations are placed in an ordered fcc configuration with the Al^{3+} anions occupying the octahedral interstitial vacancies. The nonstoichiometric-to-stoichiometric transition may therefore involve substantial rearrangement of the Al^{3+} and O^{2-} ions. In fact, there have been a number of discussions about the structure of crystalline Al_2O_3 films based on SEXAFS (Ref. 15) and photoemission¹⁷ studies. $\gamma\text{-Al}_2\text{O}_3$ or $\gamma\text{-Al}_2\text{O}_3$ -like spinel structure was almost always the proposed structure drawn from those experimental studies.

Another form of stoichiometric aluminum oxide, $\alpha\text{-Al}_2\text{O}_3$, is not thermodynamically favored under our experimental conditions.⁹ Furthermore, an EELS study by Liehr *et al.*⁴⁰ on single crystal $\alpha\text{-Al}_2\text{O}_3$ reveals a *dissimilar* set of phonon modes compared to that obtained in our stoichiometric thin film.

In view of the results of our current work, there exists the possibility that the stoichiometric aluminum oxide

film characterized by the two phonon modes in EELS is associated with the γ -Al₂O₃ (or at least with a local structure based on this atomic arrangement). Therefore it is highly desirable that a similar lattice dynamical model calculation be carried out, based on the structural arrangement in γ -Al₂O₃, in an effort to (1) bring agreement between our observed phonon spectrum and the assumed structure of γ -Al₂O₃; (2) explain from a structural standpoint the differences between the two types of aluminum oxide films and the differences in their phonon spectra; (3) as a natural result of (1) and (2), help to bring together a clear structural picture of the oxidation process.

IV. SUMMARY

The combination of EELS and AES has proven to be useful for investigating the oxidation of aluminum since these two spectroscopic methods can yield information concerning both the vibrational spectrum and the Al valence state distribution. It has been shown through our previous work⁷ that this combination provides information about the onset of oxidation of Al. In the present work, through the same combination of these two spectroscopic tools, we are able to provide the criteria for complete oxidation of Al. In both cases, there has been remarkably good agreement and correlation between the EELS and AES data.

A summary of the results of this work is now given.

(1) Aluminum oxide thin films with different extents of oxidation can be sensitively characterized by their vibrational spectrum using EELS measurements. An increasing degree of oxidation induces changes in the optical-phonon modes, leading to the loss of a 400-cm⁻¹ mode when stoichiometric Al₂O₃ is produced.

(2) Complete oxidation is reflected in the vibrational spectrum of thin Al₂O₃ films where the characteristic two-phonon-mode EEL spectrum is observed.

(3) Al-rich nonstoichiometric aluminum oxide exhibits a characteristic three-phonon-mode EEL spectrum containing the 400-cm⁻¹ vibration.

(4) Methods have been developed to efficiently cycle between stoichiometric and nonstoichiometric aluminum oxide films.

(5) Additional lattice dynamical model calculations are needed to account for the observed changes in the optical-phonon modes.

ACKNOWLEDGMENTS

We acknowledge with thanks the support of this work by the General Motors Corporation. We also acknowledge helpful discussions with Dr. Galen Fisher of the General Motors Research Laboratories.

*Also at Department of Physics, University of Pittsburgh, Pittsburgh, PA 15260.

¹H. Froitzheim, H. Ibach, and S. Lehwald, Phys. Rev. B **14**, 1362 (1976).

²T. S. Rahman, A. B. Anton, N. R. Avery, and W. H. Weinberg, Phys. Rev. Lett. **51**, 1979 (1983).

³H. Ibach and D. Bruchmann, Phys. Rev. Lett. **44**, 36 (1980); J. M. Szeftel, S. Lehwald, H. Ibach, T. S. Rahman, J. E. Black, and D. L. Mills, *ibid.* **51**, 268 (1983); T. S. Rahman, D. L. Mills, J. E. Black, J. M. Szeftel, S. Lehwald, and H. Ibach, Phys. Rev. B **30**, 589 (1984).

⁴J. M. Mundenar, A. P. Baddorf, E. W. Plummer, L. G. Sneddon, R. A. Didio, and D. M. Zehner, Surf. Sci. **188**, 15 (1987).

⁵J. L. Erskine and R. L. Strong, Phys. Rev. B **25**, 5547 (1982); R. L. Strong, B. Firey, F. W. de Wette, and J. L. Erskine, *ibid.* **26**, 3483 (1982).

⁶J. E. Crowell, J. G. Chen, and J. T. Yates, Jr., Surf. Sci. **165**, 37 (1986).

⁷J. G. Chen, J. R. Crowell, and J. T. Yates, Jr., Phys. Rev. B **33**, 1436 (1986); **35**, 5299 (1987).

⁸M. H. Mohamed, J.-S. Kim, and L. L. Kesmodel, Phys. Rev. B **40**, 1305 (1989).

⁹D. L. Cocke, E. D. Johnson, and R. P. Merrill, Catal. Rev. Sci. Eng. **26**, 163 (1984).

¹⁰H. H. Madden and D. W. Goodman, Surf. Sci. **150**, 39 (1985); S. D. Bischke, D. W. Goodman, and J. L. Falconer, *ibid.* **150**, 351 (1985).

¹¹J. G. Chen and J. T. Yates, Jr., Surf. Sci. **187**, 243 (1987); J. G. Chen, M. L. Colaianni, J. T. Yates, Jr., and G. B. Fisher, *ibid.* (to be published).

¹²D. Venus, D. A. Hensley, and L. L. Kesmodel, Surf. Sci. **199**,

391 (1988).

¹³For a review, see I. P. Batra and L. Kleinman, J. Electron Spectrosc. Relat. Phenom. **33**, 175 (1984).

¹⁴P. H. Citrin, J. E. Rowe, and S. B. Christman, Phys. Rev. B **14**, 2642 (1976).

¹⁵J. Stöhr, L. I. Johansson, S. Brennan, M. Hecht, and J. N. Miller, Phys. Rev. B **22**, 4052 (1980).

¹⁶D. Norman, S. Brennan, R. Jaeger, and J. Stöhr, Surf. Sci. **105**, L297 (1981).

¹⁷A. Bianconi, R. Z. Bachrach, S. B. M. Hagstrom, and S. A. Flodström, Phys. Rev. B **19**, 2837 (1979); A. Bianconi, R. Z. Bachrach, and S. A. Flodström, *ibid.* **19**, 3879 (1979).

¹⁸S. A. Flodström, C. W. B. Martinsson, R. Z. Bachrach, S. B. M. Hagstrom, and R. S. Bauer, Phys. Rev. Lett. **40**, 907 (1978).

¹⁹P. Hofmann, C. V. Muschwitz, K. Horn, K. Jacobi, A. M. Bradshaw, K. Kambe, and M. Scheffler, Surf. Sci. **89**, 327 (1979).

²⁰C. F. McConville, D. L. Seymour, D. P. Woodruff, and S. Bao, Surf. Sci. **188**, 1 (1987).

²¹D. E. Halverson and D. L. Cocke, J. Vac. Sci. Technol. A **7**, 40 (1989).

²²C. Ocal, S. Ferrer, and N. Garcia, Surf. Sci. **163**, 335 (1985).

²³P. K. Hansma, Phys. Rep. **30**, 145 (1977).

²⁴F. P. Mertens, Surf. Sci. **71**, 161 (1978).

²⁵J. Chatelet, H. H. Claassen, D. M. Gruen, I. Sheft, and R. B. Wright, Appl. Spectrosc. **29**, 185 (1975).

²⁶R. L. Strong, B. Firey, F. W. de Wette, and J. L. Erskine, J. Electron Spectrosc. Relat. Phenom. **29**, 187 (1983); R. L. Strong and J. L. Erskine, J. Vac. Sci. Technol. **3**, 1428 (1985).

²⁷C. Astaldi, P. Geng, and K. Jacobi, J. Electron Spectrosc. Relat. Phenom. **44**, 175 (1987).

- ²⁸J. G. Chen, J. E. Crowell, and J. T. Yates, Jr., *J. Chem. Phys.* **84**, 5906 (1986).
- ²⁹J. Paul and F. M. Hoffmann, *J. Phys. Chem.* **90**, 5321 (1986).
- ³⁰J. Paul, *J. Vac. Sci. Technol. A* **5**, 664 (1987).
- ³¹P. Brüesch, R. Kötz, H. Neff, and L. Pietronero, *Phys. Rev. B* **29**, 4691 (1984).
- ³²P. J. Chen, M. L. Colaianni, and J. T. Yates, Jr., *J. Vac. Sci. Technol.* (to be published).
- ³³J. G. Chen, M. L. Colaianni, W. H. Weinberg, and J. T. Yates, Jr. (unpublished).
- ³⁴K. G. Lynn, *Phys. Rev. Lett.* **44**, 1330 (1980).
- ³⁵M. L. Bozack, L. Muehlhoff, J. N. Russell, W. J. Choyke, and J. T. Yates, Jr., *J. Vac. Sci. Technol. A* **5**, 1 (1987).
- ³⁶C. Benndorf, H. Seidel, and F. Thieme, *Surf. Sci.* **67**, 469 (1977).
- ³⁷Similar three- to two-phonon-mode conversion has also been observed in our EELS studies through the thermal decomposition of adsorbed H₂O on an Al-rich oxide layer at elevated temperatures. It is consistent with further oxidation of the Al-rich layer by oxygen produced by the decomposition of H₂O.
- ³⁸A. G. Jackson and M. P. Hooker, *Surf. Sci.* **28**, 373 (1971).
- ³⁹The assumption that the 400-cm⁻¹ phonon mode becomes dipole inactive upon complete oxidation is not likely to be true since off-specular EELS measurements on the stoichiometric Al₂O₃ layer do not reveal any additional vibrational mode in the 400-cm⁻¹ region. The idea that the 400-cm⁻¹ mode is due to "localized" vibration of Al atoms on an Al₂O₃ lattice has also been tested by additional metal deposition studies on a stoichiometric Al₂O₃ film. With evaporated Al, Mg, Fe, and Rh on the oxide film, only Al succeeded in producing the 400-cm⁻¹ mode, and only after annealing. Thus it is unlikely that the origin of the 400-cm⁻¹ mode can be ascribed simply to the presence of surface metal atoms.
- ⁴⁰M. Liehr, P. A. Thiry, J. J. Pireaux, and R. Caudano, *J. Vac. Sci. Technol. A* **2**, 1079 (1984).